Title
PLASTIC STRESS-STRAINRATE-TEMPERATURE RELATIONS

Authors
Larsen, T.L.
Rajnak, S.L.
Hauser, F.E.
et al.

Publication Date
1963-04-30

UCRL-10789 Rev. 1

University of California

Ernest O. Lawrence Radiation Laboratory

PLASTIC STRESS-STRAINRATE-TEMPERATURE RELATIONS

Berkeley, California

DISCLAIMER

UCRL-10789 Rev. 1

J. Mechanics and Physics of Solids

UNIVERSITY OF CALIFORNIA

Lawrence Radiation Laboratory
Berkeley, California

AEC Contract No. W-7405-eng-48

PLASTIC STRESS-STRAINRATE-TEMPERATURE RELATIONS IN H. C. P. Ag-Al UNDER IMPACT LOADING

T. L. Larsen, S. L. Rajnak, F. E. Hauser
and J. E. Dorn

April 30, 1964

PLASTIC STRESS-STRAINRATE-TEMPERATURE RELATIONS IN H. C. P. Ag-Al UNDER IMPACT LOADING

T. L. Larsen, S. L. Rajnak, F. E. Hauser
and J. E. Dorn

Department of Mineral Technology and
Inorganic Materials Research Division, Lawrence Radiation Laboratory
University of California, Berkeley, California

April 30, 1964

ABSTRACT

The dynamic behavior of single crystals of Ag_2Al was investigated at strain rates from 10^{-4} to 10^{5} per sec. Basal slip was found to be almost strain-rate insensitive; the yield stress was found to increase slightly with an increase in temperature. This behavior is explained in terms of Suzuki locking. In contrast, prismatic slip was found to be very strain rate sensitive. At high temperatures and low strain rates a diffusion controlled deformation mechanism is operative which is surpressed at high strain rates giving an increase in yield strength of a factor of 30. The prismatic slip behavior is explained in terms of the Peierls mechanism of kink pair formation. The resolved shear stress for $\{10\bar{1}2\}$ twinning as a function of temperature and strain rate was also determined. Finally, the theory of plastic wave propagation is reexamined in the light of deformation rate determining dislocation mechanisms.

I. INTRODUCTION

This investigation was undertaken for the express purpose of studying the plastic behavior of single crystals under conditions of impulsive loading with specific emphasis on the significance of the dynamic behavior of dislocations to the formulation of the mathematical theory of plastic wave propagation. For this objective single crystals of the hexagonal phase Ag_2Al containing 67 atomic percent Ag and 33 atomic percent Al were selected for study because of the variety of flow rate determining dislocation mechanisms they are known to exhibit under conditions of slow deformation.[1] It will be shown that when the plastic deformation is controlled by an athermal dislocation mechanism, the deformation stress is insensitive to the strain rate and temperature. In contrast, when the motion of dislocations at low temperatures is thermally activatable, the flow stress increases with an increase in strain rate and a decrease in temperature. However at high temperatures thermally activated deformations which are dependent on diffusion are supplanted by other mechanisms when the strain rate is so high that there is insufficient time for diffusion to take place.

II. EXPERIMENTAL TECHNIQUE AND PROCEDURE

Specimen Preparation: Oriented single crystal rods of the intermetallic phase, 33 atomic percent Al-67 atomic percent Ag were grown from high purity Ag (99.995 weight percent) and Al (99.995 weight percent) in a vertical furnace under a positive argon atmosphere by the standard Bridgman technique. The rods were cut into specimens, annealed at 650°C to relieve residual stresses, and etched in nitric acid to remove the surface oxide.

For the purpose of studying the two slip systems of the hexagonal close-packed structure, specimens were oriented for basal slip by the $\{0001\}\langle 11\bar{2}0\rangle$ mechanism or for prismatic slip by the $\{\bar{1}100\}\langle 11\bar{2}0\rangle$ mechanism. Both compression and shear tests were performed. For the compression tests, cylindrical rods, one-half inch in diameter by one inch in length, were oriented for maximum resolved shear stress on the particular slip system tested as shown in Fig. 1a. As anticipated, specimens oriented for slip on the prismatic plane in the compression type test exhibited $\{10\bar{1}2\}$ twinning. For this reason shear tests, as shown in Fig. 1b, were also made. In these tests the slip plane and the Burgers vector were oriented parallel to the shearing plane. Because of the short gage section the shear tests had the added advantage of providing very high rates of shear strain, in the vicinity of more than 10^4 per sec for the dynamic tests.

Experimental Apparatus: The apparatus used to produce and measure the dynamic stresses and high strain rates, previously described in detail by Hauser and Winter[2] and Hauser, Simmons, and Dorn,[3] is shown schematically in Fig. 2. The input and output bars used in this investigation were 1/2 inch

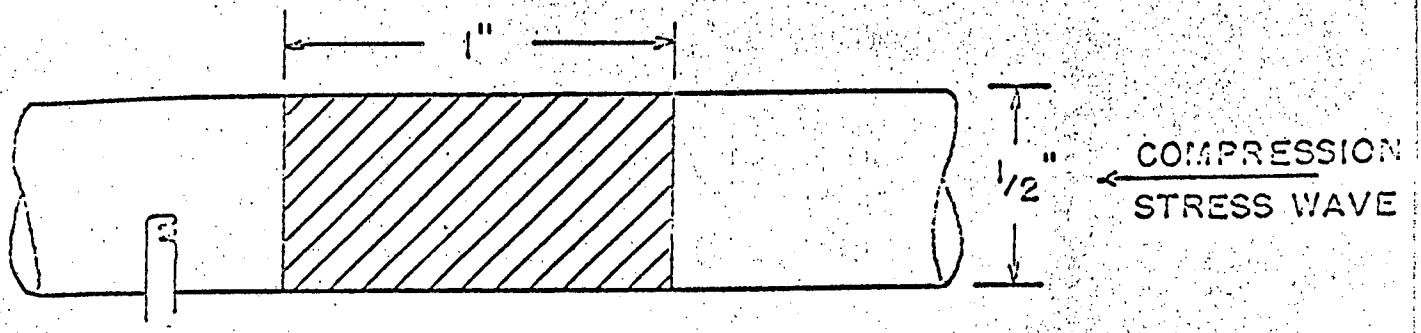

SLIP PLANE AND BURGER'S VECTOR
AT 45° TO SPECIMEN AXIS.

(a)

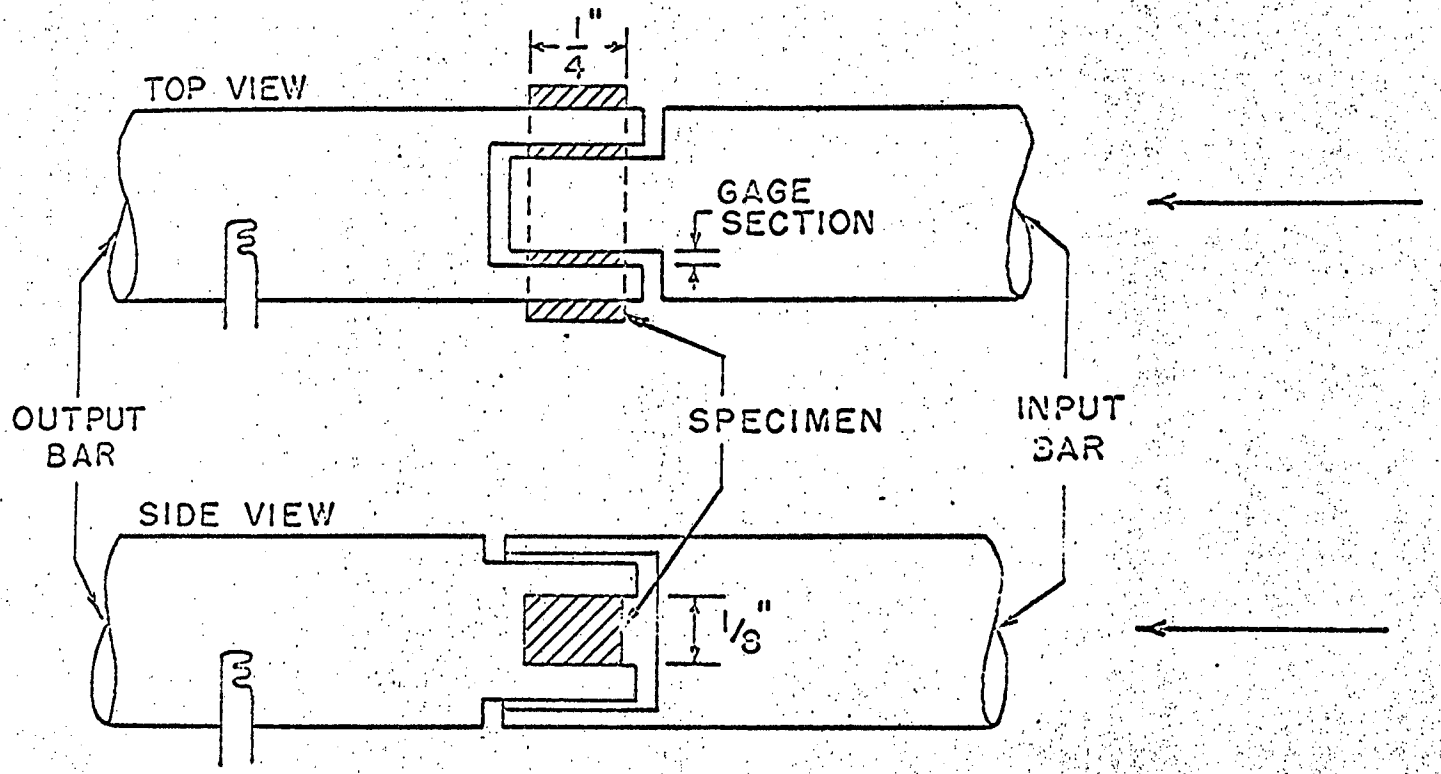

SLIP PLANE AND BURGER'S VECTOR
PARALLEL TO COMPRESSION AXIS.

(b)

FIG. 1 TESTING FIXTURES.

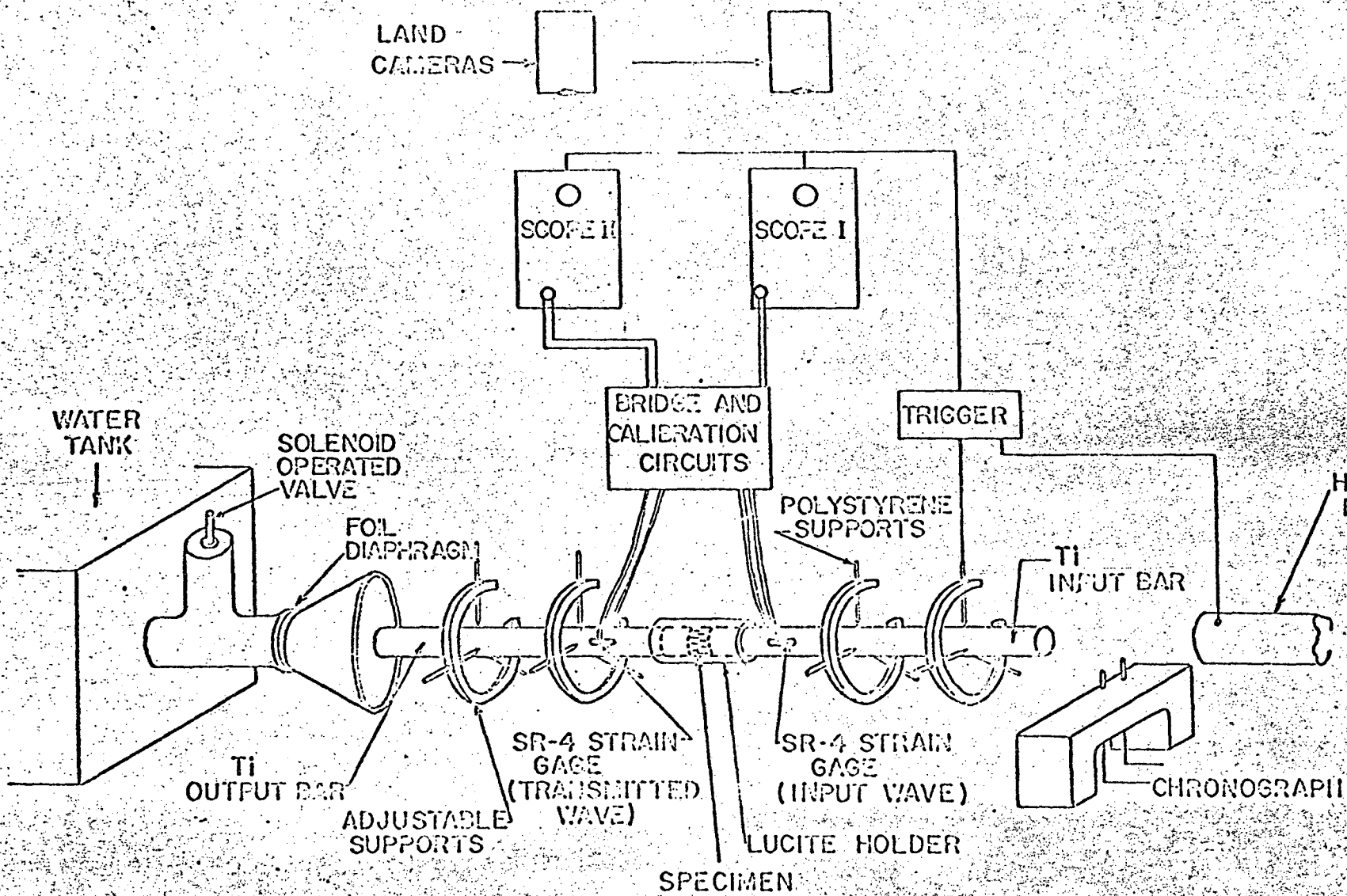

FIG. 2 EXPERIMENTAL ARRANGEMENT AND INSTRUMENTATION

MU-30752

diameter Ti-6Al-4V titanium alloy. Elevated temperatures were achieved by encasing the specimen and the ends of the bars in a small furnace. A thermocouple was attached directly to the specimen to measure the temperature. The electric strain gages on the input and output bars were water cooled and operated at room temperature.

Method of Analysis: The analysis of the dynamic compression tests by which the resolved shear stresses and shear strains were obtained followed that previously described by Hauser, Simmons, and Dorn.[3] Analogous techniques were used in the shear tests from which the shear stress on the slip plane and the shear-strain rate over the operative gage section were determined. Although the shear-type tests were introduced primarily to study prismatic slip, their accuracy was established by comparison with compression tests for basal slip. As will be shown, data obtained from the dynamic shear tests agree well with those from dynamic compression tests. Because previously reported data on Ag-Al was obtained from slow single crystal tension tests, a number of slow compression tests were carried out for purposes of comparison.

III. EXPERIMENTAL RESULTS

Basal Slip: The shear stress vs shear strain curves for basal slip at 300°K obtained from the various techniques that were employed gave almost identical average stress-strain curves. Certain minor differences, however, were apparent: whereas a single Luder's band formed in the slow tension test giving only an initial yield point, the slow compression test gave a serrated stress-strain curve suggestive of a rapid relaxation of the stress followed by either a reinitiation of the migration of the first band or the generation of a second Luder's band front, etc. It was not determined whether this difference arose as a result of a harder or stiffer compression testing procedure or as a result of the differences in stress concentration at the Luder's band front in compression as compared with tension. The dynamic compression test also revealed serrations over the first part of the test, which were much greater than those usually observed that arise exclusively from the dynamic test conditions. In contrast, the stress-strain curves obtained from the dynamic shear tests were almost free from such serrations.

The nominal identity of the resolved shear stress vs resolved shear strain curves obtained by the various techniques clearly justify the use of the dynamic shear type of tests in this case. The results of all tests for basal slip are summarized in Table I. The upper yield point was selected from the maximum initial stress level whereas the lower yield point was selected from the minimum stress level following yielding.

The resolved shear stress at the upper and lower yield strengths for basal slip are recorded in Fig. 3 as functions of temperature. Since the oxide coating has been found to affect the strength of single crystals,

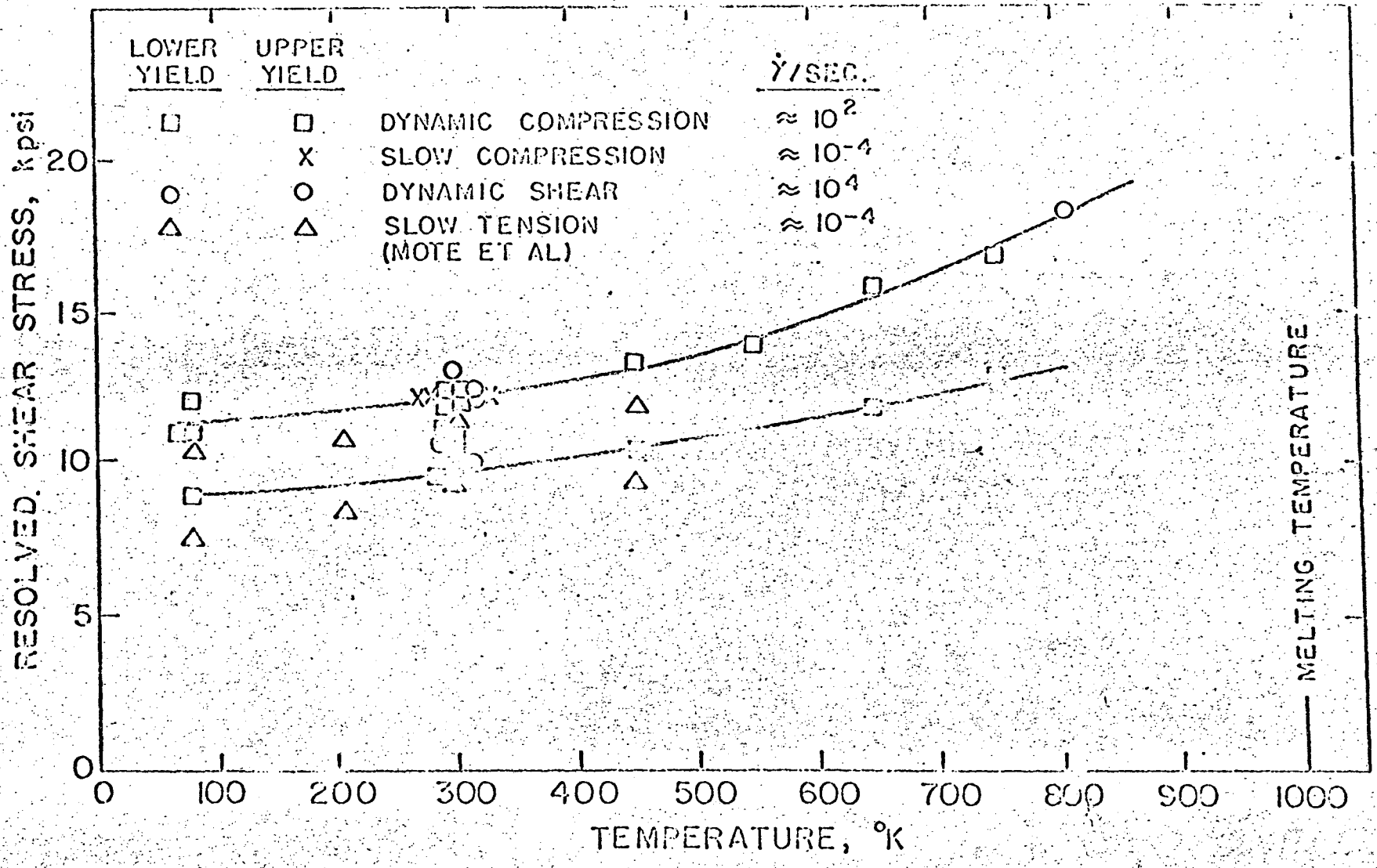

FIG. 3 RESOLVED SHEAR STRESS vs. TEMPERATURE FOR BASAL SLIP IN Ag_2Al.

MU-30754

TABLE I

YIELD STRENGTHS FOR BASAL SLIP

Type of Test*	T°K	Upper Yield K PSI	Lower Yield K PSI	Ave. Shear Strain rate/sec.
D.C.	77	11	9	820
D.C.	77	12	11	940
S.T.	77	10.6	7.5	.0004
S.T.	194	11	8.3	.0004
S.T.	300	11.5	9	.0004
D.C.	300	12.5	11	1360
D.C.	300	12	11	380
D.C.	300	12	9.5	380
D.C.	300	12.5	10.6	140
D.S.	300	12.6	10.1	45,000
D.S.	300	12.4	10.9	43,000
D.S.	300	13.2	10.1	87,000
S.C.	300	12.4	11.4	.0004
S.C.	300	12.8	12.2	.0004
S.C.	300	12.5	11.3	.0004
S.T.	450	12	9.5	.0004
D.C.	450	13.5	10.5	560
D.C.	550	14	--	340
D.C.	650	16	12	280
D.C.	750	17	13	480
D.S.	820	17.5	--	52,000

*S.T. Slow tension[1]
D.C. Dynamic compression
S.C. Slow compression
D.S. Dynamic shear

errors introduced by atmospheric testing at high temperatures were investigated. Two crystals were heat treated in air at 650°K, the oxide coating removed from one, and then both were tested at 77°K. Since the difference in stress was within the scatter of the data, any effect due to the surface oxide was discounted.

The increase in the yield strength with increasing temperature is, therefore, ascribed to the operative dislocation mechanism.

Twinning: As expected compression specimens favorably oriented for slip on the prismatic plane twinned by the operation of the two most favorably oriented $\{10\bar{1}2\}$ modes of twinning long before the resolved shear stress on the prismatic plane reached its critical value for slip. Several typical dynamic resolved shear stress-time records for twinning are reproduced in Fig. 4. Over the first regions of a test the flow stress remained substantially constant, but the curves always exhibited a rapid increase in stress level immediately following about 4% compression strain. Since the maximum compression strain for twinning alone is about 3-1/2%,[4] the data suggest that the rapid increase in stress level is due to the restraint of slip in the now twinned and, therefore, unfavorably oriented specimen. The data given in Fig. 5 refer to the possible effect of temperature on the critical resolved shear stress for twinning as deduced from the early horizontal portions of the types of records illustrated in Fig. 4. The data clearly reveal a decreasing critical resolved shear stress for twinning with increasing temperature, suggestive of a thermally activated twinning mechanism. This evidence for a thermally activated twinning mechanism is strengthened by the observation that the critical resolved shear stress for twinning increases at 77°K when the strain rate is increased.

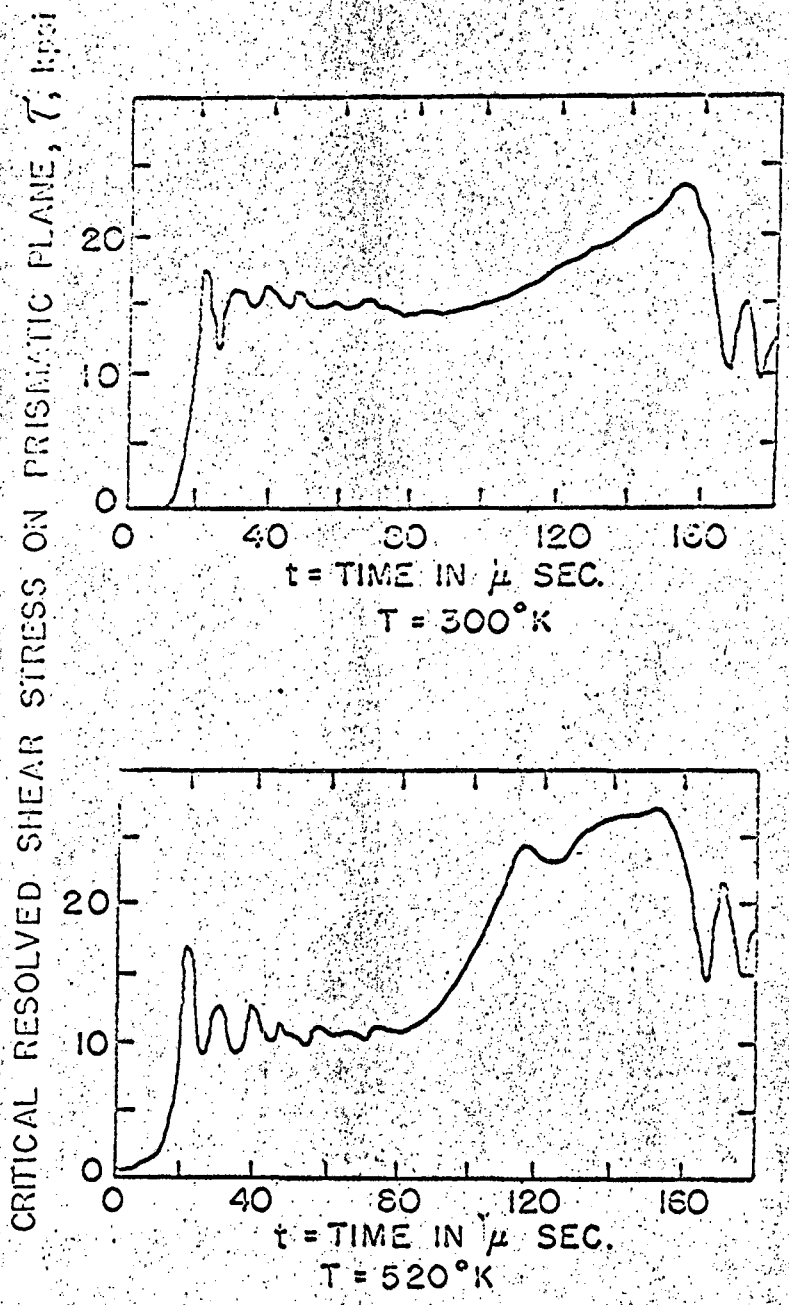

FIG. 4 RESOLVED SHEAR STRESS-TIME RECORDS FOR {10$\bar{1}$2} TWINNING IN DYNAMIC COMPRESSION OF Ag_2-Al.

MU-30755

6 G

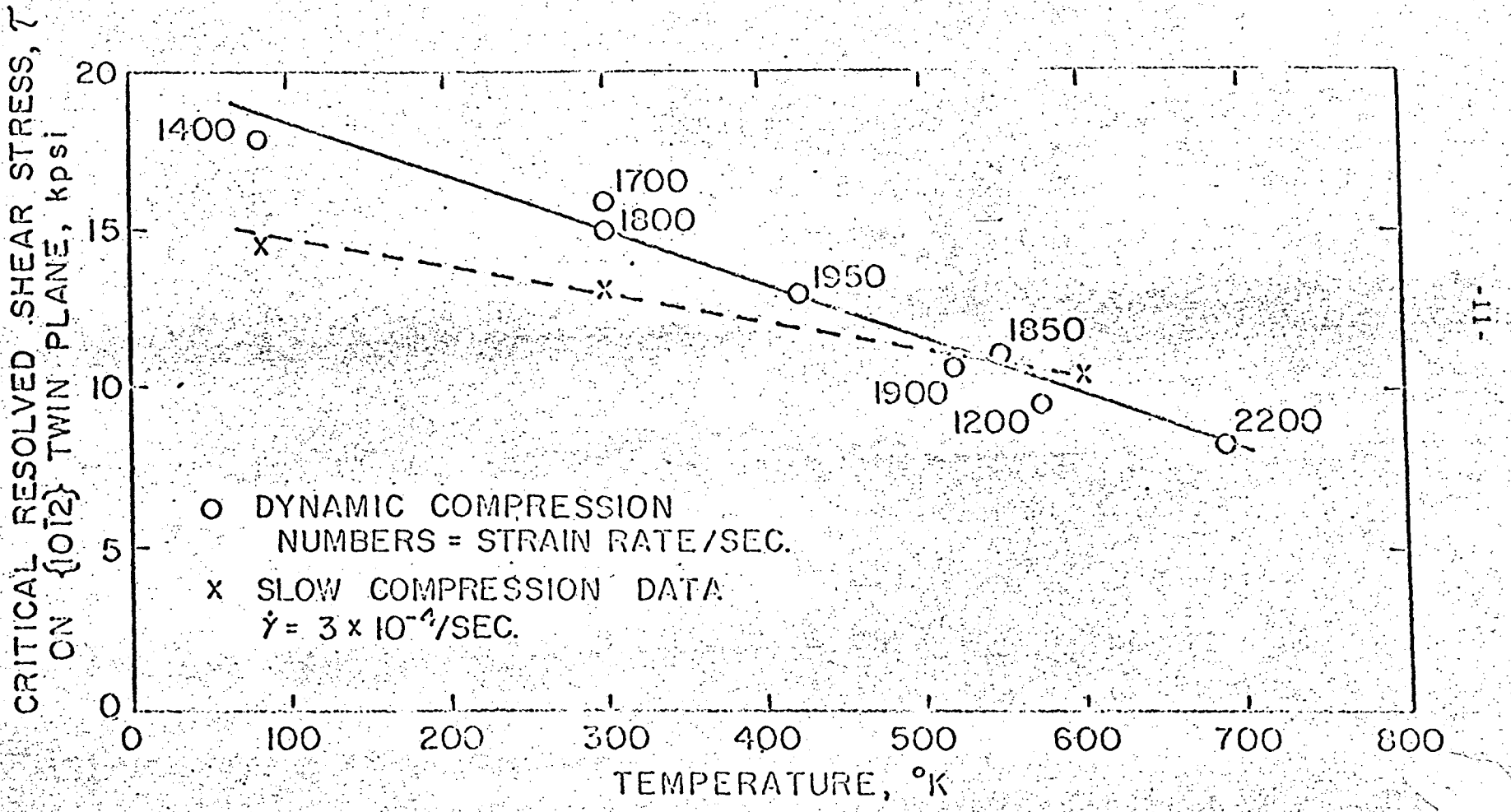

FIG. 5 CRITICAL SHEAR STRESS FOR {10$\bar{1}$2} TWINNING vs. TEMPERATURE IN Ag_2-Al.

MU-30756

One dynamic test was run in which the stress was removed after 40 μsec. This specimen was identical to those which were stressed for the full 200 μsec. in that the twins completely traversed the crystal and their average width was the same. However, there were fewer twins, indicating that the observed flow stress may be primarily due to the formations of new twins and not to the growth of existing ones. Since twinning was not a major issue for this investigation, the definitive study of twinning was postponed for more detailed future investigations.

Prismatic Slip: Because compression specimens favorably oriented for prismatic slip twinned before the critical resolved shear stress for slip was reached, the shear type tests were considered. The good agreement between the dynamic shear test data and the equivalent data that were obtained from the other types of test that were employed in studying basal slip attests to the nominal validity of the mechanics of the shear tests. All specimens that were tested in shear for prismatic slip did exhibit some microstructural evidence of twinning. But this was very small, particularly at the higher temperatures.

Typical dynamic test data for shear tests are shown in Fig. 6. Over the range of temperatures above 200°K stress-time records of the type shown in "b" of Fig. 6 were obtained which exhibited a small yield point drop followed by practically zero strain hardening with continued deformation. Specimens exhibiting this type of dynamic behavior experienced almost exclusively prismatic slip complicated with only very small amounts of localized twinning. This type of behavior was quite analogous to that obtained in the slow tension types of test where twinning was completely

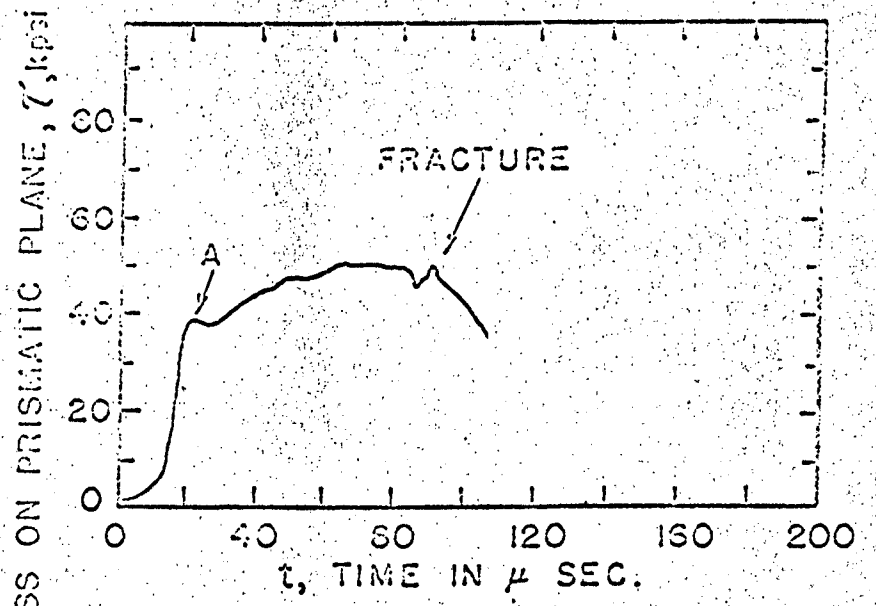

(a) T = 77 °K, $\dot{\gamma} \approx$ 20,000/SEC.

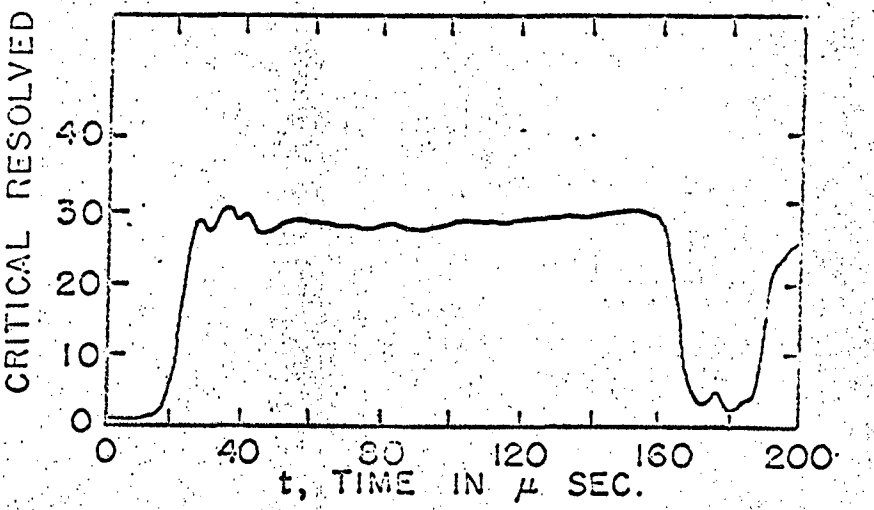

(b) T = 555 °K, $\dot{\gamma}$ = 24,000/SEC.

FIG. 6 RESOLVED SHEAR STRESS – TIME RECORD FOR PRISMATIC SHEAR TESTS IN Ag_2-Al.

MU-30757

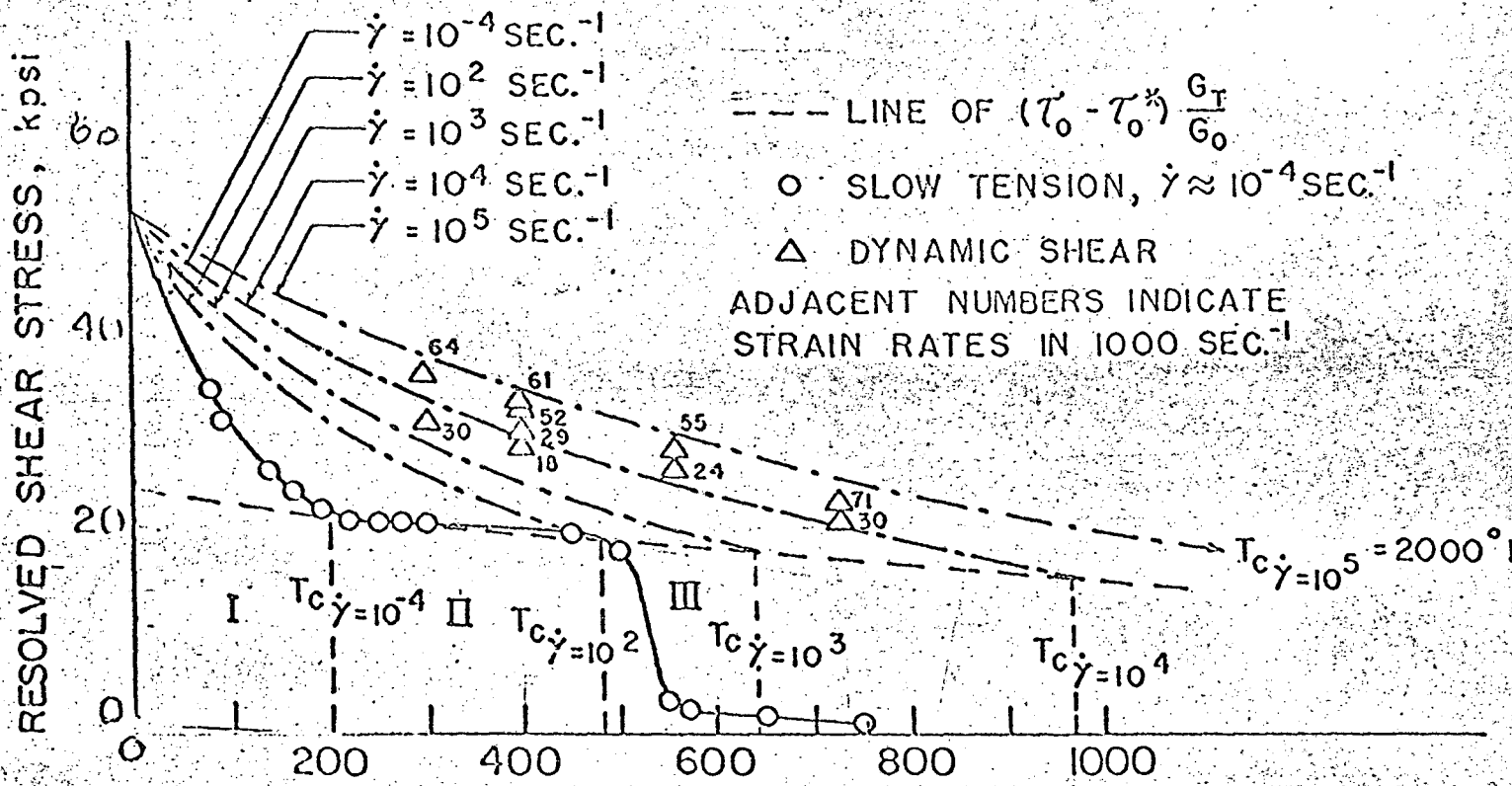

FIG. 7 RESOLVED SHEAR STRESS vs. TEMPERATURE FOR PRISMATIC SLIP IN Ag_2-Al.

absent.[1] At temperatures of 194°K and below, however, records of the type shown in "a" of Fig. 6 were obtained which exhibited considerable amounts of strain hardening. Specimens from such tests revealed considerable amounts of twinning which was evidently responsible for the strain hardening. Because of the uncertainty whether twinning or slip caused deformation, these tests were not considered in Fig. 7 and in the discussion in Section IVb. A summary of the initial yield strengths without noticable twinning for both the slow tension and dynamic shear tests as a function of temperature and strain rate are recorded in Fig. 7.

IV. DISCUSSION

A. Basal Slip

The presence of a yield point for basal slip in the Ag-33 atomic % Al alloy reveals that the dislocations that are initially present on the basal plane are locked in position. As shown in Fig. 3, the yield stress is not only insensitive to great changes in strain rate from 10^{-4} to 6×10^{4} per sec but remains substantially constant with temperature up to about 400°K and thereafter, in sharp contrast to the usual trends, it increases as the melting temperature is approached. Obviously, the operative deformation controlling dislocation mechanism is athermal. Such athermal resistance to the motions of dislocations can arise from long-range stress fields due to other dislocations, recombined dislocations, long-range order, short-range order, and Suzuki locking. Overcoming the long-range stress fields and the recombination forces will not provide a yield point and will give flow stresses that decrease linearly with an increase in temperature in a way that parallels the decrease in shear modulus of elasticity with temperature. As proposed by Flinn,[5] alloys exhibiting long-range order can exhibit strengthening with an increase in temperature up to about one-half of the melting temperature but x-ray diffraction analyses have shown that the Ag_2-Al hexagonal phase does not have long-range order. Whereas short-range order is known to be present in this alloy, the athermal yield stress for the short-range ordered alloys should decrease with an increase in temperature.[6] Having thus disqualified all other known athermal processes, we will now demonstrate that the experimental results can be rationalized in terms of Suzuki locking.

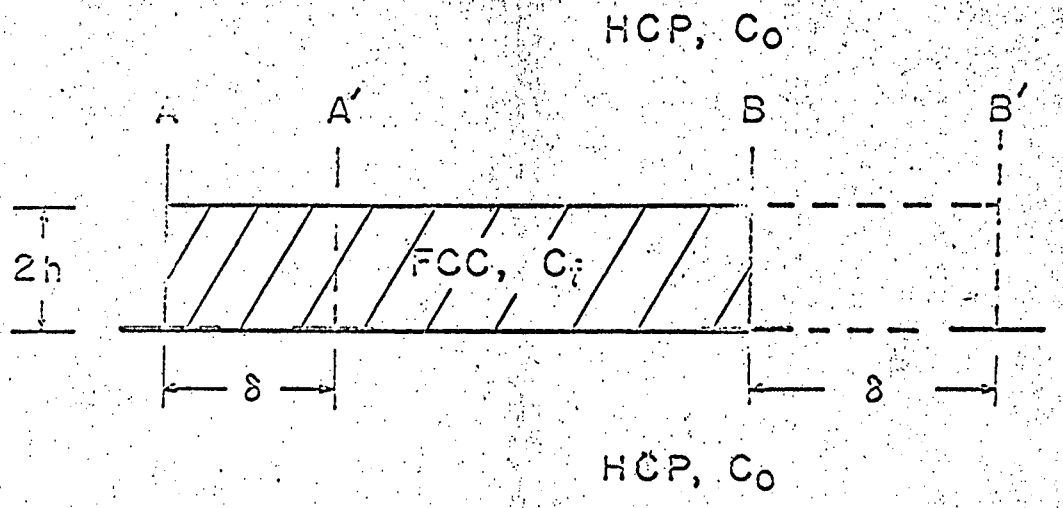

FIG. 8 STACKING FAULT ON THE BASAL PLANE OF A HCP STRUCTURE.

MU-30759

As shown in Fig. 8, when dislocations on the basal plane of a hexagonal CP structure dissociate, they form a stacking fault two atomic layers high (2h) in which the packing of layers of atoms coincides with a FCC structure. At sufficiently high temperatures (e.g. above about 0.45 of the melting temperature) where diffusion can take place, the solute atoms will distribute themselves between the stacking fault and the surrounding ideal crystal as dictated by two phase equilibrium. Because of the small fraction of the volume occupied by the stacking fault, the ideal regions of the crystal retain approximately the average composition C_o, but the composition in the stacking fault changes to C_f.

Suzuki[7] has shown that when a sufficiently high stress, τ_s, is applied in the direction of the Burgers vector, the dislocations move a distance δ, as shown in Fig. 8. From the work done by the applied stress it follows that

$$\tau_s = \frac{2h}{Vb} \left\{ (F^f - F^h)_{C_o} - (F^f - F^h)_{C_f} \right\} \qquad (1)$$

where h is the distance between adjacent slip planes, V is the molar volume of the crystal, b is the Burgers vector, F^h is the free energy per mole of the hexagonal phase and F^f is the free energy per mole of the fault. The subscripts C_o and C_f identify the compositions at which the free energies in the curved braces are to be evaluated. Since the sets of partials were originally at equilibrium, the change in free energy given in the curved braces is always positive, and consequently a positive stress is always required to move Suzuki-locked dislocations.

Two features of the above discussion are significant to the problem under consideration. First the entire length of the partial dislocations move

at the same time revealing that very high energies are required to activate the motion of Suzuki-locked dislocations. Consequently, this mechanism is athermal. Secondly, once the pair of partials have been moved past the region of composition C_f so fast that equilibrium cannot be reestablished in their new location, the subscript C_f in the last term of Eq. 1 becomes C_o. Under these conditions the stress, τ_s, becomes smaller. Therefore, a Suzuki-locked alloy will exhibit a yield point. Both of these requirements are satisfied by the data for basal slip.

It is not possible to calculate τ_s directly from Eq. 1, since the required thermodynamic data for the free energies of the faulted region are presently unknown and are not easily established. However, it is possible to show that the experimentally determined values of τ_s and the increase with temperature are certainly within the theoretically acceptable range for Suzuki locking. For this purpose we follow the development by Suzuki, assuming that the thermodynamics of both the crystal and faulted regions may be approximated by the ideal solution laws. It has been shown[7] that for this limiting approximation,

$$\tau_s = \frac{2h}{Vb} (C_o - C_f)\Delta F = (C_o - C_f) \frac{1}{b} (\gamma_{Al} - \gamma_{Ag}) , \qquad (2)$$

where C_o and C_f refer to the mole fraction of Al in the alloy and in the stacking fault respectively, γ_{Al} and γ_{Ag} are the stacking fault energies per cm^2 in pure hexagonal Al and pure hexagonal Ag respectively,

$$\Delta F = (F^f_{Al} - F^h_{Al}) - (F^f_{Ag} - F^h_{Ag}) \qquad (3)$$

where F^h_{Al} and F^h_{Ag} refer to the free energies per mole of pure hexagonal Al and pure hexagonal Ag and F^f_{Al} and F^f_{Ag} refer to the free energies

per mole in the stacking faults of pure Al and pure Ag (i.e., face-centered cubic phases). The quilibrium condition is given by

$$\frac{C_f}{1-C_f} = \frac{C_o}{1-C_o} e^{-\frac{\Delta F}{kT}} \qquad (4)$$

Introducing the experimentally determined stress at the upper yield as representative of the Suzuki unlocking stress τ_s, Eqs. 2 and 4 were solved simultaneously to give $\gamma_{Al} - \gamma_{Ag}$ as a function of temperature. Such simultaneous solutions, however, are only valid above about 400°K since the composition C_f at lower temperatures refers to the frozen-in value at about 400°K. It is for this reason that the experimentally determined τ_s is practically independent of the temperature below about 400°K.

As shown in Fig. 9, two possible sets of $\gamma_{Al} - \gamma_{Ag}$ are obtained from the experimental data. Since, however, the stacking fault energy in cubic Al is greater than that for cubic Ag, the stacking fault energy for hexagonal Al is less than that for hexagonal Ag. On this basis the solid line of Fig. 9 represents the appropriate values. Both the order of magnitude of the stacking fault energies and the linear dependency in temperature are consistent with theoretical expectations. Consequently, theory strongly supports the concept that basal slip in the hexagonal Ag-33 at. % Al alloy is controlled by Suzuki locking.

B. Prismatic Slip

As shown in Fig. 7, the yield stress for prismatic slip exhibits three distinct regions over each of which uniquely different dislocation mechanisms are operative. The flow in Region I, which is characterized by a rapidly decreasing yield stress with increasing temperature, must be controlled by a thermally activated mechanism. In view of the small activation volume

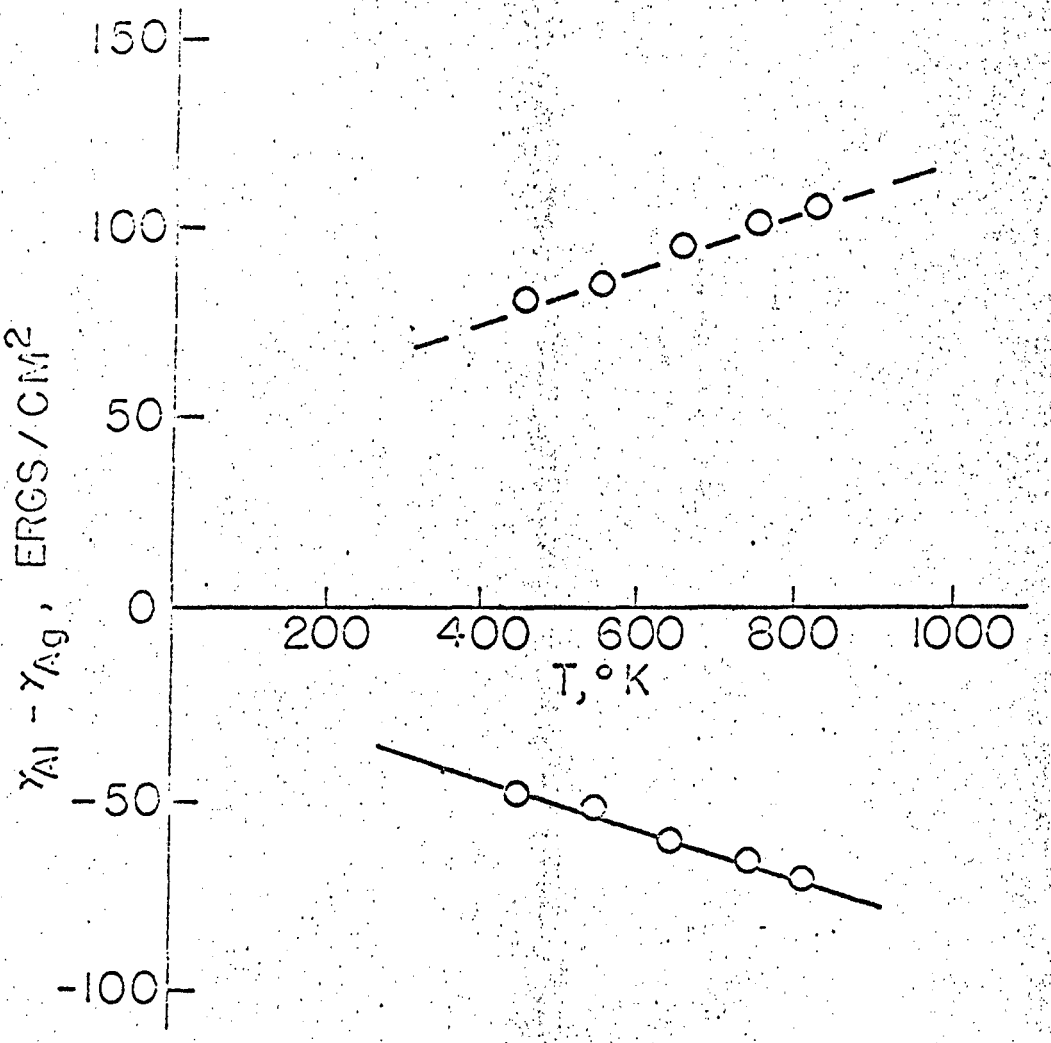

FIG. 9 STACKING FAULT ENERGIES vs. TEMPERATURE.

MU-30760

that was observed, Mote, Tanaka and Dorn[1] tentatively attributed the observed behavior in Region I to the Peierls mechanism. Over Region II the yield stress at low strain rates decreases only mildly with temperature revealing that some athermal process is operative here. These results have been shown to be wholly consistent[1] with the concept that the deformation as a result of prismatic slip in this region results from short-range order. Extensive investigation by Howard, Barmore, Mote and Dorn[8] has shown that the strain rate (or creep rate) over all of Region III can be correlated at low strain rates by the equation

$$\dot{\gamma} = 3.89 \times 10^4 \, \tau^{3.6} \, e^{\frac{-33,000}{kT}} \qquad (5)$$

where the activation energy U = 33,000 approximates that for diffusion. Consequently, at low strain rates a thermally activated diffusion controlled plastic flow process is operative over Region III.

The dynamic yield stresses recorded in Fig. 7 coincide with the usual observations on thermally activated processes, namely, than an increase in strain rate at a constant temperature leads to results equivalent to a decrease in temperature at constant strain rate. The dynamic test data, therefore, suggest that for the high strain rates encountered in the dynamic tests, the low-temperature thermally activated process is operative over all of the test temperatures that were examined. It is expected, of course, that the diffusion controlled mechanism for prismatic slip, seen in Region III, would not have time enough to be operative under high strain rates that were used in the dynamic tests. We will now demonstrate that the extent of Region I increases with an increase in strain rate and that the slow

tension test data obtained in Region I are wholly consistent with the dictates of the Peierls mechanism. Furthermore, we will show that all of the dynamic data are also in fair qualitative agreement with predictions based on the Peierls process.

Seeger,[9] Seeger, Donth and Pfaff,[10] Lothe and Hirth,[11] and Friedel[12] have discussed the Peierls mechanism. These earlier formulations of the theory, however, were only approximate and pertained accurately only for low stress levels. More recently Dorn and Rajnak[13] have completed a more rigorous and accurate theory for the Peierls process that is in excellent agreement with most of the experimental data pertaining to the Peierls mechanism in body-centered cubic metals. We will give a brief summary of this theory.

As shown in Fig. 10, the line energy of a dislocation has its minimum value when it lies parallel to certain closely packed rows of atoms. A single kink traverses the Peierls hill as shown in Fig. 10b, where as a result of its greater length, it has an energy U_k ($\approx$ the kink energy) which is greater than that of a dislocation lying exclusively in the valley. To move a dislocation lying exclusively in one valley to the next in the absence of a thermal fluctuation requires that a stress, τ_p, equal to the Peierls stress be applied. If a stress $\tau^* < \tau_p$ is applied, the dislocation, in the absence of thermal fluctuations, will move only part way up the Peierls hill as shown by the straight dislocation BB'. But at all temperatures above the absolute zero, thermal fluctuations will provide energy to form segments such as CDD'C'. Most of these will collapse back. But if the thermal fluctuation is great enough, a critical stage will be reached such that the pair of kinks so produced will move away from each other thereby

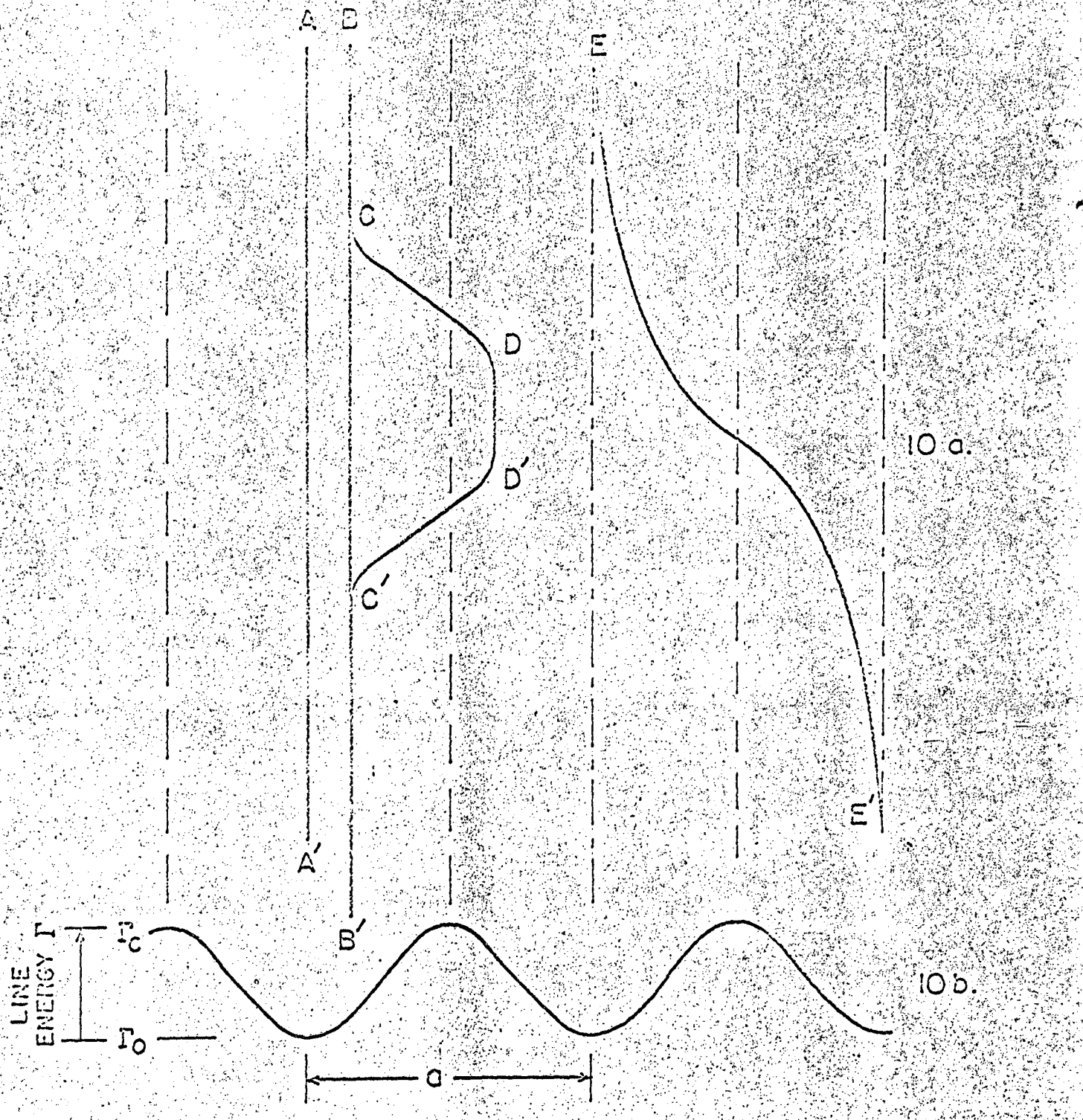

FIG. 10 PROCESS OF NUCLEATION OF A PAIR OF KINKS.

MU-30761

advancing the dislocation forward by the periodicity, a, of the lattice. The theory for the Peierls process permits an accurate determination of the saddle point energy $U_n\{\tau^*\}$ for the nucleation of a pair of kinks. On this basis the shear strain rate, $\dot{\gamma}$, is given by the Boltzmann type of formulation as

$$\dot{\gamma} = (\varrho L)\,(La)\,b\,(\nu bL/wb)\,e^{-\frac{U_n}{kT}} \qquad (6)$$

where L is the geometrically determined distance over which the pair of kinks move, ϱ is the density of the freely movable dislocations, ν is the Debye frequency, w is the width of the critical size of loop, and kT and b have their usual meaning. Equation 6, which assumes that only one pair of kinks is migrating in distance L at one time, must be replaced by a slightly more complicated relationship, as shown by Dorn and Rajnak,[13] when several kinks move at the same time in the geometric length L. Equation 6, however, will be adopted here because it predicts results in good agreement with the present experimental data.

Equation 6 is valid only up to a critical temperature, T_c, because the necessary thermal fluctuations at T_c and above are so frequent that even for an infinitesimal stress, no wait time is needed for nucleation of a pair of kinks. For this critical condition, Eq. 6 becomes

$$\dot{\gamma} = \left(\varrho\, a\, b\, \nu L/w\right) e^{-\frac{U_k}{kT_c}} \qquad (7)$$

where U_k is the kink energy. Since w appears in the pre-expoential term and is furthermore only mildly sensitive to τ^*, it can to a first approximation be treated as substantially constant. Therefore, for a given strain rate, ρ and L constant, Eqs. 6 and 7 give

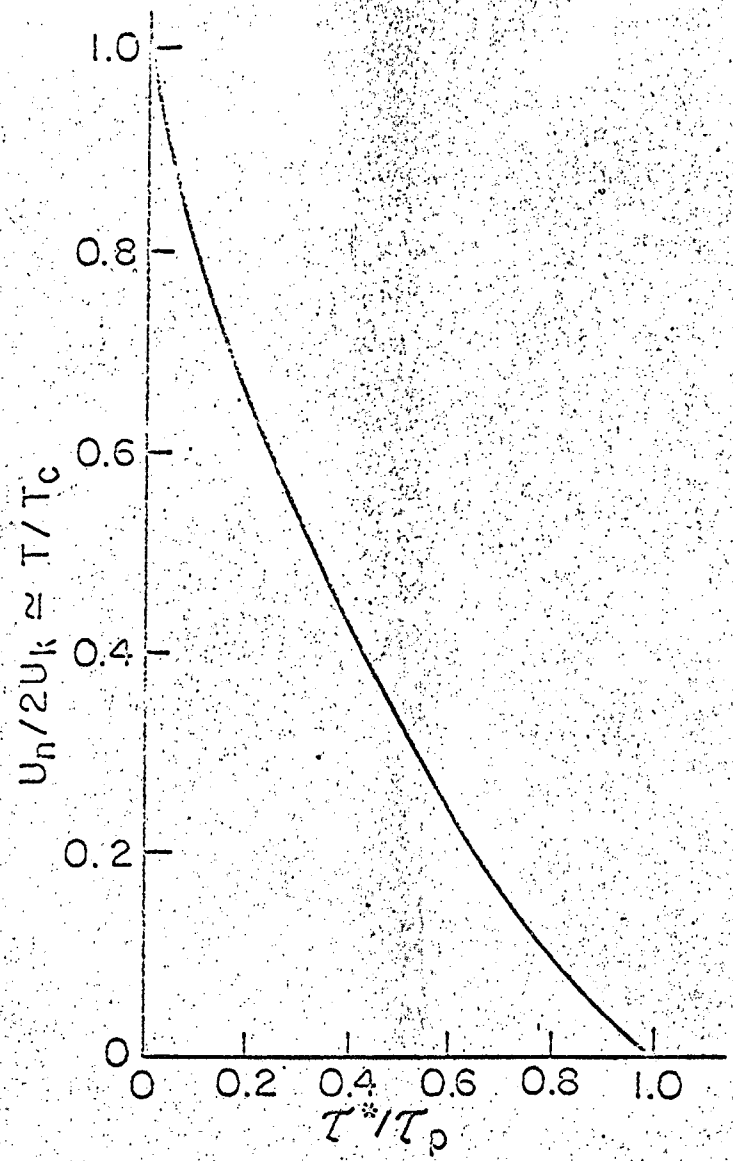

FIG. 11 DEPENDENCE OF THE ENERGY TO NUCLEATE A PAIR OF KINKS ON THE APPLIED STRESS.

$$\frac{U_n\{\tau^*\}}{2U_k} = \frac{T}{T_c} \tag{8}$$

The theoretical evaluation of $U_n/2U_k$ as a function of $\frac{\tau^*}{\tau_p}$ for the case where the Peierls hill is sinusoidal is given in Fig. 11.[13] This curve is valid for all materials: As τ^* approaches zero, the energy that must be supplied by a thermal fluctuation to produce a pair of kinks is $2U_k$. When the stress, τ^*, equals the Peierls stress, no additional energy need be supplied by a thermal fluctuation to cause the forward motion of a dislocation and U_n becomes zero. As shown by Eq. 8, the theory can be viewed in terms of τ^*/τ_p as a function of T/T_c. At the absolute zero, therefore, as shown in Fig. 11, $\tau^* = \tau_p$, whereas $\tau^* = 0$ at $T = T_c$.

The slow tension test data given in Fig. 7 can now be correlated with the theoretical predictions based on the Peierls mechanism. Neglecting the possible but small effect of temperature on the Peierls stress, we obtain the solid curve given in Fig. 7 over Region I as the theoretical curve fitted to $\tau^* = \tau_p$ at $T = 0$ and $\tau^* = 0$ at $T = T_c$.

We will now explore the dynamic test data for prismatic slip. Assuming that ρ and L were the same for the slow tension and dynamic shear tests, the theory suggests that

$$\frac{\dot{\gamma}_1}{\dot{\gamma}_2} = \frac{e^{\frac{-2U_k}{kT_{c_1}}}}{e^{\frac{-2U_k}{kT_{c_2}}}} \tag{9}$$

Using the value of $U_k = 3 \times 10^{-13}$ ergs determined by Rosen, Mote and Dorn[14] during slow tension tests in Ag_2 - Al and $T_{c_1} = 200°K$ for

$\dot{\gamma} = 10^{-4}$ sec^{-1}, the values of T_{c_2} for $\dot{\gamma} = 10^2$, 10^3, 10^4, and 10^5 can be computed using Eq. 9. The shear modules correction for Ag_2 - Al also given in reference 14 can be used to determine $\left(\frac{T}{T_c}\right)$ $\left(\frac{G_{C_T}}{G_T}\right)$ and then the corresponding $\frac{\tau^*}{\tau_p}$ can be read off Fig. 11. At T = 0, $\tau_o^* = \tau_{po}$; so from Fig. 7 where the dashed line $(\tau_o - \tau_o^*)\ \frac{G_T}{G_o}$ is drawn to a best fit through the experimental data, the value of τ_{po} = 28Kpsi can be read off. Assuming that $\tau_{pT} = \tau_{po}\ \frac{G_T}{G_o}$, τ_T^* can be evaluated and the flow stress τ plotted as a function of T for various strain rates. These theoretically predicted curves are shown in Fig. 7 for $\dot{\gamma} = 10^2$, 10^3, 10^4, and 10^5 as dash-dot lines. The experimentally determined dynamic yield stresses are shown with the adjacent numbers indicating the strain rate in 1000 sec^{-1} for each point. Considering the experimental difficulties and the necessary assumptions in the theory, the agreement is excellent.

C. Plastic Waves

All theories of plastic wave propagation are based on the equations for dynamic equilibrium and the conditions for continuity and therefore differ from each other only with respect to the constitutive equations that describe the dynamic elastoplastic behavior of the material. Using only the Hugoniot equations for equilibrium and the condition for continuity, the velocity, $\frac{d\alpha}{dt}$ of the propagation of a wave down a thin longitudinal bar is given by

$$\frac{d\alpha}{dt} = \frac{[\sigma]/[\varepsilon]}{\rho} \qquad (10)$$

where

$[\sigma]$ = the step or shock in the engineering stress,

$[\varepsilon]$ = the step or shock in the total engineering strain,

and ρ is the density of the material. For crystalline material, however, the shock in total strain, $[\varepsilon]$, can only refer to the shock in elastic strain, since the shock in plastic strain is zero. This follows because, as shown by Frank,[15] the energy per unit length, Γ, of a moving dislocation depends on its velocity v. For a screw dislocation, Γ is given by the relativistic-like equation

$$\Gamma(v) = \Gamma_o \left(1 - \left(\frac{v}{c} \right)^2 \right)^{-1/2} \qquad (11)$$

where Γ_o is the rest energy and c is the velocity of an elastic shear wave. As shown by Johnston and Gilman[16] in their investigations on LiF, the velocity of dislocations under high stress approaches the limiting value of c, as suggested by Eq. 11. Because the energy of dislocations depends on their velocity, they have inertia; and as shown by expanding Eq. 11 into a Taylor's series, for velocities less than about 0.1c the effective mass of a dislocation is about Γ_o/c^2. Consequently the instant a shock in stress arrives at a dislocation which was originally at rest, the dislocation remains at its original position but it accelerates. Because there can be no abrupt change in the position of dislocations as a result of a shock in stress, there can be no shock in plastic strain. Therefore, the shock in the total shown can only equal the shock in elastic strain and Eq. 10 always reduces to

$$\frac{d\alpha}{dt} = \sqrt{E/\rho} \qquad (12)$$

where E is Young's modulus of elasticity.

Since the inertia of dislocations is very small, they accelerate rapidly to their limiting velocity. This concept has also been experimentally verified

by Johnston and Gilman[16] who observed that the dislocations undertook the same displacement under a single stress pulse as under a series of stress pulses of the same total duration. For example, neglecting damping, the accelerative period of a dislocation can be calculated by equating the rate of work done by the stress to the increase in line energy according to

$$\tau bv = \frac{d\Gamma}{dt} \tag{13}$$

When this is integrated, taking $v = 0$ at $t = 0$, the result is

$$bct = \frac{\Gamma_o}{c^2} v \left[1 - \left(\frac{v}{c}\right)^2\right]^{-1/2} \tag{14}$$

Using the values appropriate for Al, namely $c = 5 \times 10^5$ cm/sec, $b = 2.86 \times 10^{-8}$ cm and $\Gamma_o = Gb^2/2 = 1.1 \times 10^{-4}$ ergs/cm where G is the shear modulus of elasticity, we observe that for a stress as low as $\tau = 10^8$ dynes/cm^2, a dislocation will reach 0.9c in about 2×10^{-11} sec. Furthermore, the shear strain at this time is

$$\gamma = \int_o^{2 \times 10^{-11}} \rho bv dt = 1.4 \times 10^{-4} \tag{15}$$

assuming a density of dislocations of $\rho = 10^8$ per cm^2. Approximately the same answer is given by more sophisticated analyses on the dynamic behavior of a Frank-Read source.[17] At present there is no experimental equipment available to explore this accelerative period over such short intervals of time. Furthermore, engineering interest usually centers about the much longer times of 10^{-8} sec. or greater and much higher plastic strains than about 10^{-4}. Consequently, for most types of plastic wave problems, it is appropriate to neglect the accelerative period.

For this reason the constitutive equations to be used in plastic wave propagation problems need not contain the rates of change of strain rate as would be necessary when the analysis must account for the acceleration of the dislocations.

All mechanisms of dislocation motion involve the absorption energy. Therefore as a shock passes through material, the stress level at the front of the shock is continually reduced by plastic deformation at the wave front until the stress decreases to such a low value that finally only elastic straining results at the shock front. Three classes of cases deserve consideration as shown in Table II.

Both Class I and Class II phenomena give flow stresses that depend on the strain rate; the Liebfried equation for the interaction of phonons with dislocations, however, gives only small changes in stress with strain rate. The effect of strain rate on the flow stress can be great for several of the Class II phenomenon. This is easily verified in terms of the discussion in the text of this report on the Peierls process. For both Class I and Class II processes, however, the constitutive equations must be formulated in terms of the stress and strain rate as well as the strain. And under these conditions, the plastic wave problem should be solved by means of the techniques suggested by Malvern.[18] Under dynamic conditions, however, as previously discussed, the diffusion controlled processes do not have time enough to take place and will be superseded by other mechanisms.

If over the entire low temperature range only the athermal processes of Class III are operative, the deformation stress will depend only on the strain. Suzuki locking was the example given in the text. In this event the plastic wave propagation theory can be most readily approached by the von Karman and Taylor[19] types of theory.

TABLE II

DISLOCATION MECHANISMS

Class	Name	Example	Characteristics
I	Athermal but velocity sensitive	(a) Phonon interactions with dislocations	$\dot{\gamma} = \frac{10\, e\, c\, \tau\, b^4}{3kT}$
II	Thermally activated (activation energies less than 50 kT)	(a) Peierls (b) Intersection (c) Cross-slip (d) Motion jogged screws (e) Climb of edges (f) Viscous solute atom drag	$\dot{\gamma} \propto e^{-\frac{U}{kT}}$ U depends on τ and structure and only mildly on T
III	Athermal (activation energies greater than 50 kT).	(a) Long-range stress (b) Recombination stresses (c) Short-range order (d) Long-range order (e) Suzuki locking	$\tau/G = f(\gamma)$

ACKNOWLEDGMENTS

This investigation was initally sponsored by the Lawrence Radiation Laboratory at Livermore, and more recently assigned to the Inorganic Materials Research Division of the Lawrence Radiation Laboratory in Berkeley.

This work was done under the auspices of the U.S. Atomic Energy Commission.

REFERENCES

Barrett, C. S.	1943	Structure of Metals, p. 315 (Mc-Graw Hill, Inc., New York).
Campbell, J., Simmons J. and Dorn, J.	1961	J. Appl. Mech., 83, 447.
Dorn, J., and Rajnak, S.		"Nucleation of Kink Pairs and the Peierls Mechanism of Plastic Deformation," accepted for publication Trans. AIME.
Fisher, C. A.	1954	Acta. Met., 2, 9.
Flinn, P. A.	1960	Trans. AIME, 213, 145.
Frank, F. and Read, W.	1950	Phys. Rev., 79, 722.
Friedel, J.	1962	Electron Microscopy and Strength of Crystals, (Ed. by G. Thomas and J. Washburn) p. 605 (Interscience Publishing Co.).
Hauser, F. E. Simmons, J. A. and Dorn, J.	1961	"Strain Rate Effects in Plastic Wave Propagation" in Response of Metals to High Velocity Deformation (Interscience Publishing Co.).
Hauser, F. E. and Winter, C. A.	1960	"An Experimental Method for Determining Stress-Strain Relations of High Strain Rates," University of California, MRL Pub., Series 133, Issue 4.
Howard, E., Barmore, W. Mote, J. and Dorn, J. E.	1963	Trans. AIME, 227, 1061.
Johnston, W. and Gilman, J. J.	1959	J. Appl. Phys., 30, 129.
Lothe, J. and Hirth, J. P.	1959	Phys. Rev., 115, 543.
Malvern, L. E.	1951	Quart. Appl. Math, 8, [4], 405.
Mote, J., Tanaka, K. and Dorn, J. E.	1961	Trans. AIME, 221, 858.
Rosen, A., Mote, J. D. and Dorn, J. E.	1963	University of California Lawrence Radiation Laboratory Report No. UCRL-10917.

Seeger, A.	1956	Phil. Mag., 1, 651.
Seeger, A., Donth, H. and Pfaff, F.	1957	Disc. Faraday Soc., 23, 19.
Suzuki, H.	1957	"Yield Strength of Binary Alloys," in Dislocations and Mechanical Properties of Crystals, p. 361 (J. Wiley and Sons, Inc., New York).
von Karmen, T. and Duwez, P.	1950	J. Appl. Phys., 21, 987.